JOURNAL OF GEOPHYSICAL RESEARCH, VOL. 114, G01019, doi:10.1029/2008JG000839, 2009

Landscape-scale vegetation dynamics inferred from spatial patterns of soil δ^{13}C in a subtropical savanna parkland

Edith Bai,[1,2] Thomas W. Boutton,[1] X. Ben Wu,[1] Feng Liu,[1,3] and Steven R. Archer[4]

Received 1 August 2008; revised 3 December 2008; accepted 22 January 2009; published 11 March 2009.

[1] Grasslands and savannas around the world have experienced woody plant encroachment during the past 100 years, but we know little regarding the manner in which woody plants spread across the landscape. We used soil δ^{13}C, aerial photography, and geostatistics to quantify patterns of woody encroachment in a 160 × 100 m georeferenced grid subdivided into 10 × 10 m cells in a savanna parkland landscape in southern Texas. δ^{13}C contour maps revealed that centers of closed contours coincided with centers of woody patches, and that larger woody patches developed from smaller woody plant clusters that spread laterally and coalesced. Areas where woody patches were expanding into grassland were characterized by low densities of soil δ^{13}C contour lines, and indicated the direction and extent of woody encroachment. Conversely, areas with high contour densities represented grassland-woodland boundaries that were temporally stable. Indeed, aerial photos from 1930, 1941, 1982, and 2003 confirmed that woody patches with low spatial variability in δ^{13}C corresponded to areas where woody plants had encroached during the past 30–75 years. While aerial photos can only record vegetation cover at the photo acquisition time, kriged maps of soil δ^{13}C allowed us to accurately reconstruct long-term temporal dynamics of woody plant encroachment into grassland. This approach can reliably reconstruct landscape-scale vegetation changes in areas where historical aerial photography or satellite imagery are unavailable and provides a strong spatial context for studies aimed at understanding the functional consequences of vegetation change.

Citation: Bai, E., T. W. Boutton, X. B. Wu, F. Liu, and S. R. Archer (2009), Landscape-scale vegetation dynamics inferred from spatial patterns of soil δ^{13}C in a subtropical savanna parkland, *J. Geophys. Res.*, *114*, G01019, doi:10.1029/2008JG000839.

1. Introduction

[2] Grass-dominated ecosystems in many regions around the world have experienced increased woody plant abundance during the past 100 years [*Archer et al.*, 2001; *Asner et al.*, 2004; *van Auken*, 2000]. This woody plant encroachment has long been a concern of land managers and ecologists [*Fisher*, 1950, 1977; *Rappole et al.*, 1986] because it has the potential to profoundly influence grassland biodiversity, commercial livestock grazing, hydrology, biogeochemistry and landscape evolution [*Boutton et al.*, 1999; *Nobel*, 1997; *Rappole et al.*, 1986], and could impact ecosystem services and the livelihoods of almost 20% of the world's population [*Turner et al.*, 1990]. In addition, current estimates suggest that woody plant encroachment may result in the sequestration of 0.10–0.13 Pg C a^{-1} in the USA alone, which represents 20–40% of the current U.S. carbon sink strength [*Houghton et al.*, 2000; *Tilman et al.*, 2000; *Pacala et al.*, 2001]. If these estimates are correct, then woody encroachment is certainly playing a significant role in the global C cycle and perhaps the climate system. Despite the global significance of this land cover change, we know relatively little regarding the pattern and extent of this vegetation change.

[3] In the Rio Grande Plains of southern Texas, subtropical woodlands dominated by C_3 plants have become significant components of landscapes that were once almost exclusively dominated by C_4 grasslands [*Archer et al.*, 1988; *Boutton et al.*, 1998]. Historical accounts suggest that this conversion began in the mid to late 1800s [*Johnston*, 1963] and coincided with the intensification of livestock grazing and fire suppression [*Archer*, 1995; *Archer et al.*, 2001]. In this region, small discrete woody clusters organized around a central honey mesquite (*Prosopis glandulosa*) tree, and larger groves of woody vegetation (apparently comprised of clusters that have grown together and fused) are embedded in an herbaceous matrix in uplands. The size, cover and density of woody plants are influenced by interactions between rainfall and disturbance (herbivory and fire) as constrained by soils [*Archer*, 1995; *House et al.*, 2003; *Rodriguez-Iturbe et al.*, 1999; *Scholes and Archer*, 1997].

[1]Department of Ecosystem Science and Management, Texas A&M University, College Station, Texas, USA.
[2]Now at Department of Land, Air, and Water Resources, University of California, Davis, California, USA.
[3]Now at Forest Landscape Ecology Laboratory, Department of Forest and Wildlife Ecology, University of Wisconsin-Madison, Madison, Wisconsin, USA.
[4]School of Natural Resources, University of Arizona, Tucson, Arizona, USA.

0148-0227/09/2008JG000839$09.00

[4] Previous studies suggested that the increases of woody cover were initiated by the establishment of honey mesquite, an unpalatable, stress-tolerant N_2-fixing tree. As mesquite trees establish and grow, they serve as recruitment foci, facilitating the recruitment and establishment of other woody species beneath their canopies [*Archer et al.*, 1988; *Archer*, 1995]. Studies conducted at the La Copita Research Area (situated in the eastern portion of the Rio Grande Plains of southern Texas) have shown this initiation of new shrub clusters and the expansion of established clusters increased woody cover by 150–338% since the 1940s [*Archer*, 1995; *Archer et al.*, 2001]. However, we still know little about the successional processes that lead to the development of increased woody plant cover in grass-dominated ecosystems. Understanding vegetation dynamics at the landscape scale will aid in reconstruction of patterns of woody plant encroachment in the past, and will help us predict future changes which may occur on landscapes not only in this region, but in other grass-dominated regions around the world where woody encroachment is prevalent.

[5] The natural abundance of stable carbon isotopes in soil can be utilized to document changes in ecosystem structure wherever C_3 plants are encroaching into C_4 dominated ecosystems, or vice versa [*Dzurec et al.*, 1985; *Jessup et al.*, 2003; *Krull et al.*, 2005; *Derner et al.*, 2006; *Dumig et al.*, 2008]. C_3 and C_4 plants have unique $\delta^{13}C$ values which are incorporated into the soil without significant fractionation during soil organic carbon formation [*Boutton*, 1996; *Boutton et al.*, 1998; *Fernandez et al.*, 2003; *Wedin et al.*, 1995]. In the Rio Grande Plains of southern Texas, all woody plants have the C_3 photosynthetic pathway ($\delta^{13}C \approx -27‰$) and all grasses have the C_4 pathway ($\delta^{13}C \approx -13‰$) [*Boutton et al.*, 1999]. Therefore, soil $\delta^{13}C$ values reflect the relative contributions of plant species with C_3 and C_4 photosynthetic pathways to community net primary productivity, and should be useful in reconstructing this vegetation change from C_4 grassland to C_3 woodland. The difference between the isotopic composition of the current plant community and that of the soil organic matter created by the vegetation change will persist for a length of time determined by the soil organic matter turnover rate [*Boutton et al.*, 1998]. Previous studies have demonstrated the usefulness of $\delta^{13}C$ natural abundance for documenting vegetation change and estimating soil organic carbon turnover rate [*Balesdent et al.*, 1987; *Bernardes et al.*, 2004; *Krull and Bray*, 2005; *Liao et al.*, 2006]. However, most of these previous studies were conducted at the ecosystem level and were not spatially explicit. The use of quantitative spatial methods (e.g., geostatistics) in conjunction with soil $\delta^{13}C$ analyses should be a powerful approach for extending isotopic analyses of vegetation dynamics to the landscape scale; however, these methodologies have been merged in only two previous studies [*Biggs et al.*, 2002; *van Kessel et al.*, 1994].

[6] Use of satellite images or aerial photographs to study woody plant encroachment and the spatial pattern of vegetation have received increased attention [*Archer et al.*, 2004; *Fensham and Fairfax*, 2003; *Laliberte et al.*, 2004; *Witt et al.*, 2006]. However, aerial photos are seldom available prior to 1935, and satellite images useful for discerning vegetation dynamics at the landscape scale are generally not available prior to about 1980 [*Loveland and DeFries*, 2004]. If spatial patterns of soil $\delta^{13}C$ can accurately reconstruct the dynamics of woody plant encroachment, they can supplement, enhance, or serve in lieu of aerial photos or satellite imagery to yield direct evidence for the successional development of woody patches and provide a strong spatial context for studies aimed at understanding the functional consequences of this change in landscape structure. Therefore, in this study, we used $\delta^{13}C$ values of soil organic matter in conjunction with sequential aerial photography and geostatistics to quantify the landscape-scale vegetation dynamics in the Rio Grande Plains of southern Texas. Our objectives were to: (1) Quantify spatial variation of soil $\delta^{13}C$ across the landscape; (2) Reconstruct historical vegetation cover and estimate the direction of woody plant expansion using soil $\delta^{13}C$ kriging maps; and (3) Predict the future evolution of the landscape based on results from objectives 1 and 2.

2. Study Area

[7] Research was conducted at the Texas AgriLife La Copita Research Area in Jim Wells County, 15 km SW of Alice, TX (27° 40′ N; 98° 12′ W; elevation 80m) in the eastern Rio Grande Plains of the Tamaulipan Biotic Province. The climate is subtropical with a mean annual temperature of 22.4°C and mean annual precipitation of 680 mm. Rainfall maxima occur in May–June and September.

[8] The landscape grades (1–3% slopes) from sandy loam uplands to clay loam and clay lowlands and elevations range from 75 to 90 m. This study was confined to upland portions of the landscape. Upland soils are primarily Typic Argiustolls with a subsurface argillic horizon; however, patches of Typic Haplustepts lacking an argillic horizon are also found in the uplands [*Archer*, 1995]. The vegetation is subtropical savanna parkland comprised of a grassland matrix, with discrete woody clusters (comprised of a single mesquite tree with up to 15 understory tree/shrub species, 3–10 m diameter), and larger groves (comprised of several woody clusters that have fused together, 10 to >20 m diameter) embedded within that matrix. The grasslands consist mainly of rhizomatous and weakly caespitose C_4 grasses, and C_3 forbs. Clusters and groves are dominated by *P. glandulosa* and *Zanthoxylum fagara* (lime pricklyash). Mesquite and several other leguminous trees and shrubs present in wooded areas are capable of symbiotic N_2 fixation [*Zitzer et al.*, 1996]. *Bai et al.* [2008] presented detailed biological characteristics of the dominant woody plants. *Archer* [1995] and *Boutton et al.* [1998] have additional details on soils, vegetation, and climate.

3. Methods

3.1. Study Design and Soil Sampling

[9] A 100 m × 160 m plot consisting of 10 m × 10 m grid cells was established on an upland landscape (Figure 1) which included all of the upland landscape elements: clusters, groves, and grasslands. Elevations within the study area were determined by terrain surveying and kriging interpolation. Ground control points (n = 48) were established throughout the study area, and their exact locations determined by GPS. The relative elevation of one point (Point A) was set at 0 m. The elevation change from one control point

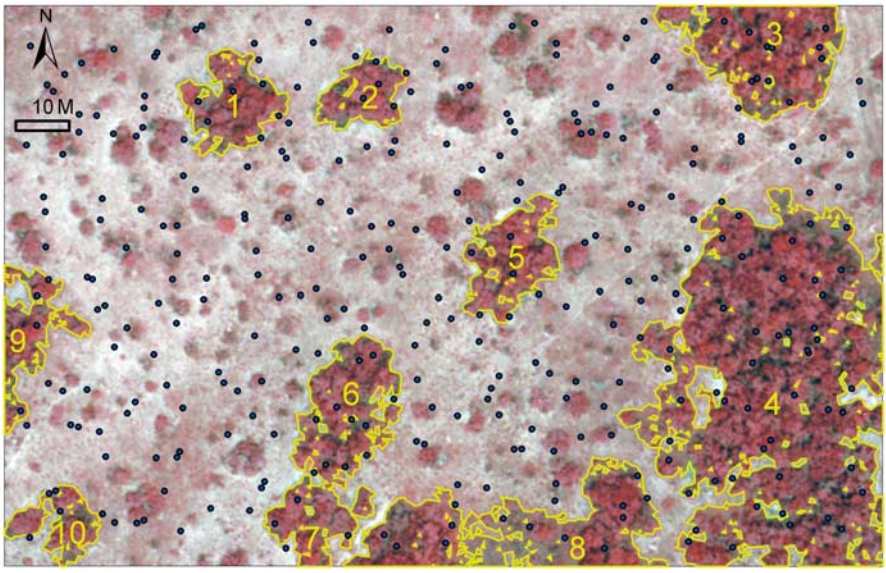

Figure 1. Color-infrared aerial view of study area. Red areas represent woody vegetation, while light gray areas represent grasslands. Blue dots indicate soil sampling locations within the 100 × 160 m grid. Numbered woody patches were evaluated in detail for evidence of expansion in size over time. Yellow lines indicate the edge of woody patches.

to another was measured by field surveying. The absolute elevation of Point A was determined on USGS 1:24,000-scale 10-m resolution DEM in UTM projection. Then the absolute elevations of the other ground control points were calculated based on their elevations relative to point A. A topographic map was developed using kriging interpolation based on the elevations of the ground control points in ArcView GIS Spatial Analyst [*Environmental Systems Research Institute* (*ESRI*)*, Inc.*, 1998].

[10] In January 2003, soil samples were collected at two points selected randomly within each cell, yielding a total of 320 sample points within the grid. All grid sampling points were generated in a GIS and located in the field using GPS. At each sample point, two soil cores (15 cm deep × 2.24 cm in diameter) were taken within 10 cm of each other; one core was utilized to determine the relative proportions of sand, silt, and clay by the pipet method [*Gee and Bauder*, 1986], while the other core was utilized to determine $\delta^{13}C$ of soil organic carbon. Soil sampling was limited to the 0–15 cm depth increment because mean residence times for soil organic carbon at this depth range from 36 to 52 years [*Boutton et al.*, 1998, 1999, 2008], which is appropriate for capturing changes in soil $\delta^{13}C$ values resulting from relatively recent C_3 woody plant encroachment into C_4 grassland. In contrast, soil organic matter at depths >15 cm has mean residence times >150 years, and $\delta^{13}C$ values at these depths largely reflect the legacy of the C_4 grassland that once dominated this site [*Boutton et al.*, 1998, 1999, 2008].

3.2. Soil $\delta^{13}C$ Analyses

[11] Soils were passed through a 2 mm sieve to remove coarse organic fragments and gravel, dried at 60°C for 48 h, and ground in a centrifugal mill (Angstrom, Inc., Belleville, MI). Ground soils were treated with HCl vapor in a desiccator to remove carbonates [*Harris et al.*, 2001], dried, and analyzed to determine the $\delta^{13}C$ of soil organic matter using a Carlo Erba EA-1108 interfaced with a Delta Plus isotope ratio mass spectrometer operating in continuous flow mode (ThermoFinnigan, San Jose, CA).

[12] Carbon isotope ratios are presented in δ notation:

$$\delta = [(R_{SAMPLE} - R_{STD})/R_{STD}] \times 10^3. \quad (1)$$

where R_{SAMPLE} is the $^{13}C/^{12}C$ ratio of the sample and R_{STD} is the $^{13}C/^{12}C$ ratio of the VPDB standard [*Coplen*, 1996]. Precision of duplicate measurements was 0.1‰ for $\delta^{13}C$.

3.3. Aerial Photography and Image Analysis

[13] Black and white aerial photos taken in 1930, 1941 and 1982 and a color-infrared (IR) aerial photo taken in 2003 were used to examine changes in vegetation cover. Aerial photos were scanned, georeferenced in UTM projection (1 m resolution), and subjected to an unsupervised classification using ERDAS Imagine [*ERDAS, Inc.*, 1998]. Forty classes were first generated based on reflectance value similarities of pixels. These classes were further grouped into two categories (woody versus nonwoody) and areas of the woody patches were calculated in ArcView GIS Spatial Analyst [*ESRI, Inc.*, 1998]. Ten woody patches comprised of multiple mesquite trees and other woody species whose present area is more than 100 m^2 (Figure 1 and Table 1) were selected as representative of invading woody patches to study the relationship between soil $\delta^{13}C$ values and vegetation dynamics revealed by sequential aerial photography. Normalized Difference Vegetation Index (NDVI) [*Rouse et al.*, 1973] of the color-infrared (IR) aerial photo taken in 2003 was calculated as (NIR − RED)/(NIR + RED), in which RED and NIR stand for the spectral reflectance measurements acquired in the red and near-infrared regions, respectively. Areas covered by woody plants have higher

Table 1. Area of the Woody Patches (Groves) in 1930 and 2003[a]

ID	Area in 1930 (m^2)	Area in 2003 (m^2)
1	181.7	227.0
2	105.7	148.9
3	227.9	475.7
4	1257.6	2330.3
5	116.8	246.6
6	240.6	348.1
7	143.4	183.1
8	206.0	631.0
9	88.3	181.8
10	91.0	131.7

[a]Units in m^2. ID numbers correspond to numbered woody patches in Figures 1, 4, and 6.

NDVI values compared to grass/bare soil area [*Scanlon et al.*, 2002].

3.4. Statistical Analysis and Mapping

[14] Descriptive statistical analyses, correlations, and regressions were performed using SPSS for Windows, version 11.5 [*SPSS, Inc.*, 2002]. Dutilleul's modified *t* tests were conducted using PASSAGE [*Rosenberg*, 2001]. Variogram analyses were conducted using VARIOWIN [*Pannatier*, 1996]. All GIS analyses were conducted using ArcView GIS Spatial Analyst [*ESRI, Inc.*, 1998]. Variogram analysis was used to determine the spatial autocorrelation pattern for soil $\delta^{13}C$ and for soil clay content. The experimental semivariogram for the lag distance h was calculated according to:

$$\gamma(h) = \frac{1}{2N(h)} \sum_{i=1}^{i=N(h)} [Z(X_i) - Z(X_{i+h})]^2 \qquad (2)$$

where $Z(x_i)$ and $Z(x_{i+h})$ are the values of measured properties at spatial location x_i and x_{i+h}, N(h) is the number of pairs with lag distance h. The model we chose was the spherical model. Nugget variance (C_0), range (A), structure variance (C) and sill ($C_0 + C$) were the parameters used to interpret spatial structure (Figure 2). The variance at lag distance zero, called ''nugget'' variance, is caused by measurement error or variation at scales smaller than the sampling unit. Usually semivariance increases with lag distance and then levels off to a constant value called the sill. The lag distance at which the sill is approached is called the range of the spatial continuity. Beyond the range, the properties can be considered spatially unrelated. The difference between the sill and the nugget is called the structural variance. The ratio of the structural variance and sill, representing the proportion of the total variance explained by the spatial structure, reveals the structure strength [*Dent and Grimm*, 1999]. Kriging was used in ArcView GIS [*ESRI, Inc.*, 1998] for spatial interpolation of values at unsampled locations based on sample data and their spatial structure determined using variogram analysis.

[15] Pearson product-moment correlation coefficients were determined between soil $\delta^{13}C$, soil clay content, elevation, and NDVI. Because spatial autocorrelation in environmental variables affects the classical tests of significance of correlation and regression coefficients, the statistical significance of these relationships was determined by Dutilleul's modified *t* test [*Legendre et al.*, 2002] which accounts for the effects of spatial autocorrelation.

4. Results

4.1. Elevation and Soil Texture

[16] Elevation within the sample grid was highest at the northeast corner (90.67 m) and lowest at the southwest corner (87.93 m), resulting in a gentle northeast to southwest slope (Figure 3a). Both clay and silt concentrations in the soil (0–15 cm) increased by approximately 100% from the north toward the south, while the concentration of the sand fraction decreased by approximately 22% in this same direction (Figures 3b–3d). The omnidirectional semivariogram analysis indicated that clay content was spatially autocorrelated over a range of 120 m, suggesting that spatial patterns of this variable are controlled by landscape processes operating at scales comparable to or larger than our sample grid. Although clay tended to be higher at lower elevations in this landscape, elevation and clay content were not correlated (Table 2).

4.2. Descriptive Statistics for Soil $\delta^{13}C$ Values

[17] Soil $\delta^{13}C$ values (0–15 cm) beneath both clusters and groves had a mean of −21.10‰, while those beneath grassland patches averaged −18.98‰ (Table 3). The mean values of soil $\delta^{13}C$ beneath woody clusters and grove patches were higher than those of the current organic matter inputs (−26 to −28‰ [*Boutton et al.*, 1998; *Bai et al.*, 2008]), indicating a proportion of soil carbon beneath present C_3 woodlands was derived from C_4 grasses.

[18] Soil $\delta^{13}C$ values in grasslands, clusters, and groves were negatively skewed, indicating the median was less than the mean with a long tail of small values to the left (Table 3). However, in general, skewness values are near zero, indicating an approximately symmetric distribution. Coefficients of variation for soil $\delta^{13}C$ values were 4.90% in grasslands, 11.56% in cluster patches, and 7.82% in groves (Table 3). The wider range of $\delta^{13}C$ in cluster and grove patches (9.56‰ and 8.68‰) also indicated that heterogeneity of soil $\delta^{13}C$ is greater beneath woody plant cover.

4.3. Spatial Patterns of Soil $\delta^{13}C$ Values and Their Potential Controls

[19] Variogram analysis was performed to assess spatial structure of soil $\delta^{13}C$ values from the 0–15 cm depth

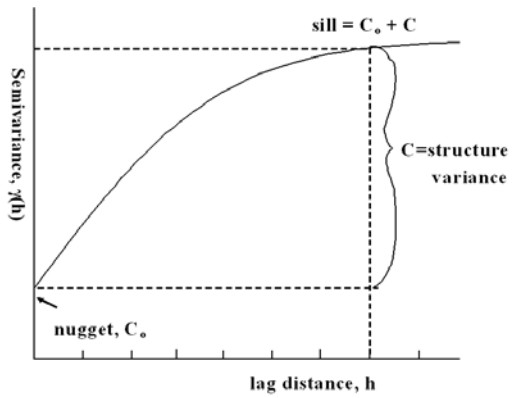

Figure 2. Components of a semivariogram.

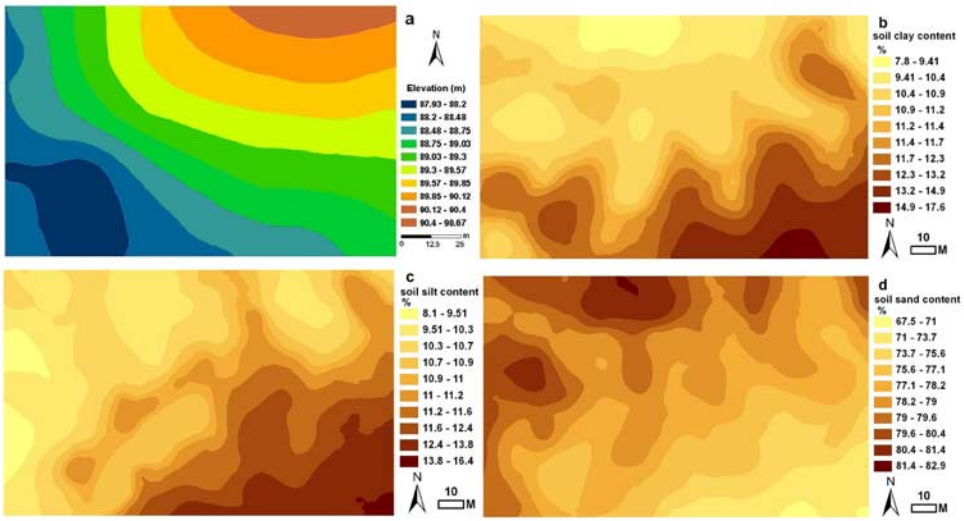

Figure 3. (a) Elevation map computed from field survey, and kriged maps of (b) soil clay, (c) silt, and (d) sand particle size fractions for the 120 × 100 m upland grid at La Copita Research Area in southern Texas. Soil particle size distributions are for the 0–15 cm depth increment of the soil profile.

interval (Table 4). Because elevation within the grid was higher at the northeast corner and lower at the southwest corner (Figure 3a), we used omni-directional, 45° from north (i.e., parallel to slope), and 135° from north (i.e., perpendicular to slope) directional models to examine if topography caused differences in spatial patterns of soil δ^{13}C. All models were spherical with a clear limit of spatial correlation (range). The range of the omni-directional model was 12.6 m, which means that there was no spatial autocorrelation of soil δ^{13}C beyond this distance. The proportion of the sill explained by spatial dependence [(sill – nugget)/sill], which indicates the strength of spatial structure at the sampling scale, was 70.3% for the omni-directional model. Soil δ^{13}C had an anisotropic spatial pattern, with stronger spatial structure [(sill-nugget)/sill = 95.7%] and shorter range (11.90 m) in the 45° direction (parallel to slope) and weaker spatial structure [(sill-nugget)/sill = 57.5%] and longer range (19.09 m) in the 135° direction (perpendicular to slope). Although this anisotropic pattern appeared to be related to slope direction, elevation was not correlated with soil δ^{13}C (Table 2). In addition, clay content was not correlated with soil δ^{13}C (Table 2).

[20] Ordinary kriging based on the variogram analysis provided estimates of soil δ^{13}C values for the 0–15 cm depth increment at locations which had not been sampled, enabling us to develop a map of soil δ^{13}C values across this landscape. When the kriged map of soil δ^{13}C (Figure 4) is compared visually with aerial photos of the study area (Figure 5), it is obvious that soil δ^{13}C values in woody patches are lower than those in grassland patches. In fact, soil δ^{13}C values were highly correlated ($p < 0.001$) with the NDVI derived from the aerial photo of 2003 (Table 2).

Table 2. Pearson Product-Moment Correlation Coefficients (r) Between Soil δ^{13}C, Elevation, Soil Clay Content, and NDVI[a]

	Elevation (m)	Clay Content (%)	NDVI
Soil δ^{13}C (‰)	0.15	0.05	−0.52***
Elevation (m)		−0.31	0.08
Clay content (%)			0.08

[a]Statistical significance of correlation coefficients was evaluated using Dutilleul's modified *t* test [*Legendre et al.*, 2002] that accounts for spatial autocorrelation within the data sets. *** $p < 0.001$.

4.4. Patterns of Woody Patch Development

[21] A contour map of soil δ^{13}C values for the 0–15 cm depth increment (Figure 6) obtained by ordinary kriging revealed the development of woody patches. Centers of concentric contour lines may represent centers of woody patches. Woody patches 1, 2, 3, 5, 6, 7, 9 and 10 each contained one contour center. Patches 4 and 8 both appear to have developed from at least three discrete smaller patches based on the existence of three obvious isotopic centers in each of those wooded areas (Figure 6). Indeed, aerial photos confirmed that patches 4 and 8 each evolved from three discrete patches between 1930 and 2003 (Figure 5).

[22] Woody plant expansion into grassland causes a reduction in soil δ^{13}C values as C_3 woody plant carbon is added to a pool of soil organic matter derived largely

Table 3. Descriptive Statistics of Soil δ^{13}C Values for the 0–15 cm Depth Under Different Types of Vegetation Cover[a]

	Grassland	Cluster	Grove
Mean	−18.98	−21.10	−21.10
Median	−18.90	−21.15	−21.52
Minimum	−23.31	−26.59	−25.81
Maximum	−16.48	−17.03	−17.13
Standard error	0.07	0.45	0.21
Standard deviation	0.93	2.44	1.65
Coefficient of variation	4.90%	11.56%	7.82%
Sample variance	0.87	5.96	2.72
Skewness	−1.07	−0.00	−0.22
Range	6.83	9.56	8.68

[a]Per mil versus VPDB.

Table 4. Parameters for Best Fitted Semivariogram of Soil $\delta^{13}C$ for the 0–15 cm Depth

	Model	Range (m)	Nugget (‰)	Sill (‰)	(Sill – Nugget)/Sill (%)
Omni-directional	spherical	12.60	0.62	2.09	70.3
45°	spherical	11.90	0.11	2.58	95.7
135°	spherical	19.09	0.71	1.67	57.5

from C_4 grasses. The change in soil $\delta^{13}C$ values should be greatest near the oldest central portion of a woody patch, and least near the grassland-woody patch boundary, resulting in concentric contour lines on the kriged map of $\delta^{13}C$ values (Figure 6). High densities of contour lines (high gradient steepness) means there is an abrupt boundary with respect to soil $\delta^{13}C$ values. Therefore, areas with high contour densities represent grassland- woodland boundaries that have been relatively stable over time. Conversely, areas where woody patches are encroaching into grassland should have low densities of soil $\delta^{13}C$ contour lines (low gradient steepness). For example, patches 2 and 7 appear to have been relatively stable given their higher densities of contour lines near their boundaries with grassland (Figure 6). In contrast, woody cover appears to have increased significantly in patches 4 and 8 based on lower densities of contour lines near their boundaries with grassland (Figure 6). Raster calculations based on aerial photos taken in 1993 and 2003 showed that woody cover of patch 7 increased only 28% while that of patches 4 and 8 increased 85% and 206%, respectively (Table 1).

[23] The asymmetric shapes of the concentric contour lines of each patch indicate the anisotropic expansion of the cluster. In other words, each patch may have variable growth rates in different directions. Denser contour lines of soil $\delta^{13}C$ near the edges of woody patches represent slower woody invasion into grassland, while sparser contour lines represented faster woody plant expansion. We estimated the direction of fastest woody expansion for each patch by selecting the direction with sparsest contour lines and indicated them by arrows starting from the center of the contour lines (Figure 6). Because patches 4 and 8 had more than one contour center, they had 3 and 2 arrows, respectively. Patch 1 appears to be expanding rapidly to the southeast and patch 2 appears to be expanding rapidly to the southwest, suggesting that they may coalesce in the future. Patch 4 was the result of coalescence of three expanding discrete clusters, which had different directions of expansion. Patch 7 was relatively stable with the least woody expansion. Patch 8 was formed by coalescence of three smaller patches. Densities of contour lines indicated that left and lower right ones expanded rapidly to northwest; while the upper left one remained relatively stable (Figure 6).

[24] To assess our inferences about the speed and direction of woody patch expansion based on soil $\delta^{13}C$ contour lines, we compared our $\delta^{13}C$-based inferences with the directions of vegetation changes computed from aerial photos taken in 1930 and 2003 (Figure 6). Directions of woody patch expansion based on soil $\delta^{13}C$ were similar to the expansion directions revealed by aerial photography for patches 1, 2, 4, 6, 7, and 8. Directional changes inferred from $\delta^{13}C$ for patches 9 and 10 were not clearly substantiated by the aerial photos; however, these patches were located on the edge of the study area and were therefore sampled incompletely. Aerial photos indicated patches 3 and 5 expanded largely around the edge in all directions.

5. Discussion

5.1. Overall Landscape Pattern of Soil $\delta^{13}C$

[25] Descriptive statistics revealed that grassland soils (0–15 cm) had a $\delta^{13}C$ value (mean ± SE) of −18.98 ± 0.07‰, while cluster and grove soils had $\delta^{13}C$ values of −21.10 ± 0.45 ‰ and −21.10 ± 0.21‰, respectively (Table 2). These values were consistent with previous studies in the same area [*Boutton et al.*, 1998, 1999; *Liao et al.*, 2006]. These data indicated that at least some of the spatial variability of soil $\delta^{13}C$ was related to vegetation cover, and that variability was slightly higher in the woody patches than in the grassland. However, spatial statistics are needed to further explore the nature of this variability.

[26] The omni-directional variogram analysis showed that the range of soil $\delta^{13}C$ was 12.6 m, indicating that values were no longer autocorrelated at distances >12.6 m. Similarly, in one of the few geostatistical studies of spatial variability of soil $\delta^{13}C$, *Marriott et al.* [1997] found that the patch size of soil $\delta^{13}C$ in a temperate grassland was 13.5 m based on variogram models. In the present study, soil $\delta^{13}C$ had an anisotropic spatial pattern, with stronger spatial structure [(sill-nugget)/sill = 95.7%] and shorter range (11.90 m) parallel to the slope and weaker spatial structure [(sill-nugget)/sill = 57.5%] and longer range (19.09 m) perpendicular to the slope (Table 4). Although these data suggest that topography (or one of its correlates) could be influencing the spatial pattern of soil $\delta^{13}C$, there was no direct correlation between elevation and soil $\delta^{13}C$ (Table 2).

[27] Topography could potentially impact $\delta^{13}C$ values of soil organic carbon by influencing soil texture, which can regulate plant community composition [*McAuliffe*, 1994] and soil organic matter turnover rates [*Jolivet et al.*, 2003; *Telles et al.*, 2003]. The clay fraction is particularly important in determining soil organic carbon turnover rates

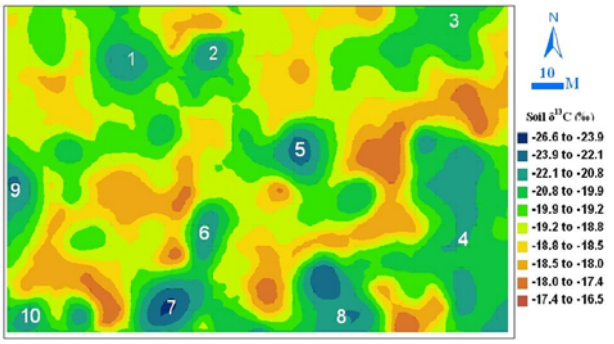

Figure 4. Kriged map of soil $\delta^{13}C$ (‰) for the 0–15 cm depth increment of the soil profile in the 120 × 100 m upland grid at La Copita Research Area in southern Texas.

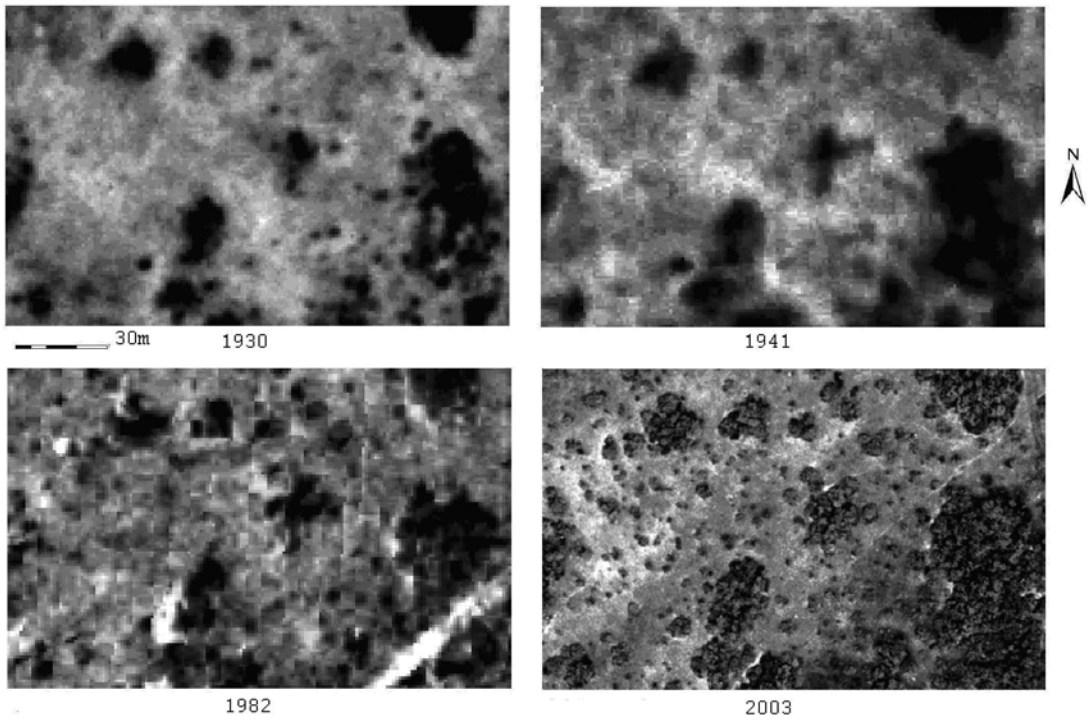

Figure 5. Aerial photos taken in 1930, 1941, 1982, and 2003 illustrate vegetation cover change for the 120 × 100 m upland grid at La Copita Research Area in southern Texas. Lighter areas are herbaceous vegetation; darker areas are woody vegetation.

through its role in the formation of stable organomineral complexes and the formation of microaggregates [*Kaiser and Guggenberger*, 2003; *McCarthy et al.*, 2008]. At the spatial scale of our study, soil clay content was not correlated with either elevation or soil δ^{13}C (Table 2). However, the strong correlation between soil δ^{13}C and NDVI may mask any potential relationship between clay and δ^{13}C. In an effort to factor out the influence of NDVI, the correlation between δ^{13}C and the residuals of the regression of clay against NDVI was evaluated. This correlation was not sig-

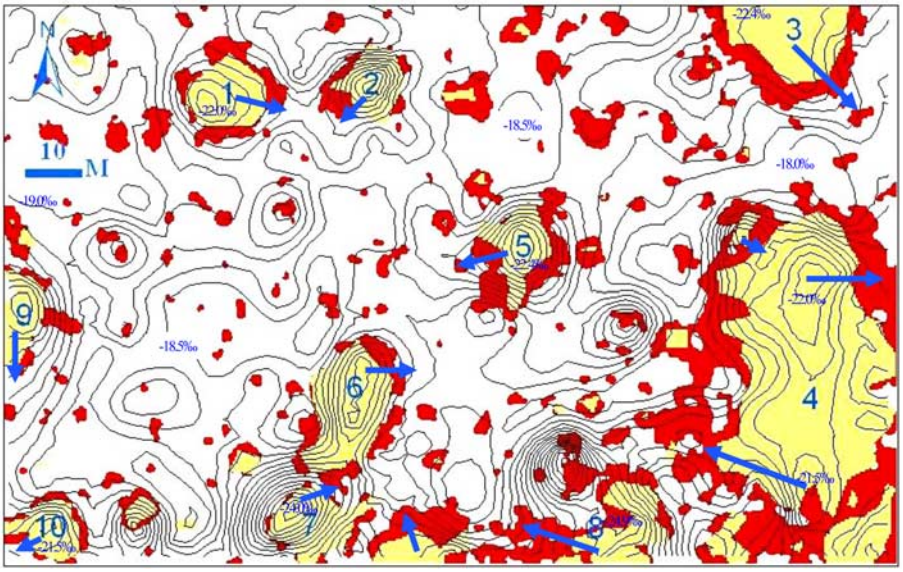

Figure 6. Soil δ^{13}C contours (at 0.4‰ intervals) for the 0–15 cm depth interval superimposed on the vegetation change map calculated from aerial photos for the 120 × 100 m upland grid at La Copita Research Area in southern Texas. Red color represents increase in woody plant cover from 1930 to 2003. Yellow color represents woody vegetation cover in 1930. Arrows suggest the direction in which woody plant cover appears to be increasing at the most rapid rate in each patch.

nificant (data not shown), further substantiating that clay content has no apparent role in explaining spatial patterns of $\delta^{13}C$ values of organic carbon in the upper 15 cm of the soil profile at the landscape scale. This does not rule out the possibility that clay content may influence soil $\delta^{13}C$ at smaller spatial scales, or that subsurface clay content may influence the $\delta^{13}C$ of surface soils through effects on plant community composition.

[28] Visual assessment of the kriged map of soil $\delta^{13}C$ (Figure 4) and aerial photographs (Figures 1 and 5) revealed the strong resemblance between the spatial pattern of soil $\delta^{13}C$ and vegetation cover. Also, correlation analysis revealed that soil $\delta^{13}C$ was negatively correlated with NDVI, such that areas with lower soil $\delta^{13}C$ values corresponded to areas with C_3 woody plant cover. These findings are consistent with previous studies documenting the strong controlling effects of C_3-C_4 plant cover on soil $\delta^{13}C$ variability [*Biggs et al.*, 2002; *van Kessel et al.*, 1994].

5.2. Formation of Wooded Landscape Elements Revealed by Soil $\delta^{13}C$

[29] Previous studies have hypothesized that the groves, larger woody patches in the upland savanna, were formed through coalescence of expanding discrete clusters [*Archer*, 1995; *Scanlan and Archer*, 1991; *Wu and Archer*, 2005]. In this study, the kriged map of soil $\delta^{13}C$ and the sequential aerial photographs both provided strong evidence in support of the proposed mechanism of grove formation by coalescence of clusters (Figure 6). Previous studies at La Copita Research Area proposed that rates of cluster development and patterns of distribution were regulated by subsurface (>15 cm) variations in clay content and by variations in annual rainfall [*Archer*, 1995; *Scanlan and Archer*, 1991]. Therefore, each woody patch may have variable growth rates in different directions due to the influences of edaphic and hydrological factors. In our study, we found the asymmetric shapes of the concentric contour lines indicated the anisotropic expansion of clusters. *McAuliffe* [1994] found edaphic features such as soil texture controlled the vertical movement and distribution of soil water, in turn affecting the distribution of woody plants in arid and semiarid environments. *Archer* [1995] suggested variations in annual rainfall and subsurface clay content (>15 cm) might regulate the rate of woody expansion. *Wu and Archer* [2005] suggested that rainfall, topography and soil texture were factors potentially influencing woody cover changes. However, the exact mechanism of the anisotropic expansion of woody clusters is still unclear. Therefore, contour maps of soil $\delta^{13}C$ may provide a strong spatial context for future studies aimed at understanding the factors regulating the rates of cluster development and patterns of woody plant distribution.

5.3. Future Landscape Evolution

[30] Landscape-scale analyses of soil $\delta^{13}C$ may also afford glimpses of future landscape evolution. Some of the present discrete clusters appear destined to coalesce and form larger groves. For example, patches 1 and 2 seem likely to coalesce because they are actively expanding toward each other, as revealed by the contour map of soil $\delta^{13}C$ (Figure 6). Some woodland margins have been relatively stable over the past 50–70 years, indicating that the grasslands at those margins may continue to remain open in the future. Simulations using transition probabilities suggested the present landscape may develop into closed-canopy woodland within the next 180 years [*Archer*, 1995]. *Wu and Archer* [2005] suggested in order to accurately predict the future rate and pattern of changes in woody abundance, rainfall-topography-soil texture relationships and scale-dependent mechanisms needed to be considered. Our study confirmed that different woody patches may have different expansion rates in the future.

[31] These results could also have implications for ecosystem management practices aimed at controlling woody plant abundance in grasslands. Because the fate of faster growing pioneer clusters may have a greater impact on woody cover increases than the establishment of new clusters [*Scanlan and Archer*, 1991], removal of faster growing clusters may slow or reverse the trend toward a closed-canopy woodland in the future.

6. Conclusions

[32] Woody plant cover has increased since the 1930s in the Rio Grande Plains of southern Texas. Geostatistical analyses showed that soil $\delta^{13}C$ values in the 0–15 cm depth increment were autocorrelated within a range of 12.6 m. Spatial patterns of soil $\delta^{13}C$ were strongly related to vegetation (primarily woody versus grassland cover), but were not correlated with elevation or soil texture at the scale examined. A contour map of soil $\delta^{13}C$ confirmed that the large upland groves were formed in the past by coalescence of expanding discrete clusters, and revealed that some clusters are currently growing rapidly toward each other and might coalesce into groves in the near future. This pattern of woody patch development was substantiated by sequential aerial photographs taken during the past 80 years. Kriged maps of soil $\delta^{13}C$ allowed us to reliably reconstruct landscape-scale spatial pattern and temporal dynamics of woody plant encroachment into grassland, suggesting this approach can be applied to reconstruct changes in woody cover in areas where historical aerial photography or satellite imagery are not available. These kriged maps of soil $\delta^{13}C$ can also provide a strong spatial context for future studies aimed at understanding the functional consequences of this change in landscape structure. The marriage of soil $\delta^{13}C$ analyses with geostatistical methods and aerial photography represents a powerful approach for studying vegetation dynamics at the landscape scale, and can be employed in any ecosystem where C_3-C_4 vegetation changes have occurred. We suggest that it may be feasible to expand this approach to the regional scale by employing similar techniques in conjunction with satellite imagery.

[33] **Acknowledgments.** This work was supported by the NSF Ecosystem Studies Program (DEB-9981723). In addition, both E. Bai and F. Liu were supported by Regents Fellowships and Tom Slick Fellowships from Texas A&M University. We are grateful to Kirk Jessup, Lisa Alexander, Donna Prochaska, Terri Rosol, Andrew Boutton, and Heather Jahnsen for assistance with field work and laboratory analyses. We thank C. Tom Hallmark and Fred E. Smeins whose constructive comments helped improve the manuscript. Thanks are also extended to David McKown, manager of the La Copita Research Area, for assistance with on-site logistics.

References

Archer, S. (1995), Tree-grass dynamics in a *Prosopis*-thorn scrub savanna parkland: Reconstructing the past and predicting the future, *Ecoscience*, *2*, 83–89.

Archer, S., C. Scifres, and C. R. Bassham (1988), Autogenic succession in a subtropical savanna: Conversion of grassland to thorn woodland, *Ecol. Monogr.*, *58*, 111–127.

Archer, S., T. W. Boutton, and K. A. Hibbard (2001), Trees in grasslands: Biogeochemical consequences of woody plant expansion, in *Global Biogeochemical Cycles in the Climate System*, edited by E.-D. Schulze et al., pp. 115–138, Academic, San Diego, Calif.

Archer, S., T. W. Boutton, and C. McMurtry (2004), Carbon and nitrogen accumulation in a savanna landscape: Field and modeling perspectives, in *Global Environmental Change in the Ocean and on Land*, edited by M. Shiyomi et al., pp. 359–373, TerraPub, Tokyo.

Asner, G. P., A. J. Elmore, L. P. Olander, R. E. Martin, and A. T. Harris (2004), Grazing systems, ecosystem responses, and global change, *Annu. Rev. Environ. Resour.*, *29*, 261–299.

Bai, E., T. W. Boutton, F. Liu, X. B. Wu, and S. R. Archer (2008), Variation in woody plant $\delta^{13}C$ along a topoedaphic gradient in a subtropical savanna parkland, *Oecologia*, *156*, 479–489.

Balesdent, J., A. Mariotti, and B. Guillet (1987), Natural ^{13}C abundance as a tracer for studies of soil organic matter dynamics, *Soil Biol. Biochem.*, *19*, 25–30.

Bernardes, M. C., et al. (2004), Riverine organic matter composition as a function of land use changes, Southwest Amazon, *Ecol. Appl.*, *14*, 263–279.

Biggs, T. H., J. Quade, and R. H. Webb (2002), $\delta^{13}C$ values of soil organic matter in semiarid grassland with mesquite (*Prosopis*) encroachment in southeastern Arizona, *Geoderma*, *110*, 109–130.

Boutton, T. W. (1996), Stable carbon isotope ratios of soil organic matter and their use as indicators of vegetation and climate change, in *Mass Spectrometry of Soils*, edited by T. W. Boutton and S. I. Yamasaki, pp. 47–82, Marcel Dekker, New York.

Boutton, T. W., S. R. Archer, A. J. Midwood, S. F. Zitzer, and R. Bol (1998), $\delta^{13}C$ values of soil organic carbon and their use in documenting vegetation change in a subtropical savanna ecosystem, *Geoderma*, *82*, 5–41.

Boutton, T. W., S. R. Archer, and A. J. Midwood (1999), Stable isotopes in ecosystem science: Structure, function and dynamics of a subtropical Savanna, *Rapid Commun. Mass Spectrom.*, *13*, 1263–1277.

Boutton, T. W., J. D. Liao, T. R. Filley, and S. R. Archer (2008), Belowground carbon storage and dynamics accompanying woody plant encroachment in a subtropical savanna, in *Soil Carbon Sequestration and the Greenhouse Effect*, *SSSA Spec. Publ*, vol. 57, 2nd ed., edited by R. Lal and R. Follett, pp. 181–205, Soil Sci. Soc. of Am., Madison, Wis.

Coplen, T. B. (1996), New guidelines for reporting stable hydrogen, carbon, and oxygen isotope-ratio data, *Geochim. Cosmochim. Acta*, *60*, 3359–3360.

Dent, C. L., and N. B. Grimm (1999), Spatial heterogeneity of stream water nutrient concentrations over successional time, *Ecology*, *80*, 2283–2298.

Derner, J. D., T. W. Boutton, and D. D. Briske (2006), Grazing and ecosystem carbon storage in the North American Great Plains, *Plant Soil*, *280*, 77–90.

Dumig, A., P. Schad, C. Rumpel, M. F. Dignac, and I. Kogel-Knabner (2008), *Araucaria* forest expansion on grassland in the southern Brazilian highlands as revealed by ^{14}C and $\delta^{13}C$ studies, *Geoderma*, *145*, 143–157.

Dzurec, R. S., T. W. Boutton, M. M. Caldwell, and B. N. Smith (1985), Carbon isotope ratios of soil organic matter and their use in assessing community composition changes in Curlew Valley, Utah, *Oecologia*, *66*, 17–24.

Environmental Systems Research Institute (ESRI), Inc. (1998), *Working with Arcview spatial analyst*, Redlands, Calif.

ERDAS, Inc. (1998), *Using Arcview image analysis*, Atlanta, Ga.

Fensham, R. J., and R. J. Fairfax (2003), Assessing woody vegetation cover change in north–west Australian savanna using aerial photography, *Int. J. Wildland Fire*, *12*, 359–367.

Fernandez, I., N. Mahieu, and G. Cadisch (2003), Carbon isotope fractionation during decomposition of plant materials of different quality, *Global Biogeochem. Cycles*, *17*(3), 1075, doi:10.1029/2001GB001834.

Fisher, C. E. (1950), The mesquite problem in the southwest, *J. Range Manage.*, *3*, 60–70.

Fisher, C. E. (1977), Mesquite and modern man in southwestern North America, in *Mesquite: Its Biology in Two Desert Ecosystems*, edited by B. B. Simpson, pp. 177–188, Dowden Hutchinson Ross, New York.

Gee, G. W., and J. W. Bauder (1986), Particle-size analysis, in *Methods of Soil Analysis, Part I, Physical and Mineralogical Methods*, edited by A. Klute, pp. 383–411, Soil Sci. Soc. of Am., Madison, Wis.

Harris, D., W. R. Horwath, and C. van Kessel (2001), Acid fumigation of soils to remove carbonates prior to total organic carbon or carbon −13 isotopic analysis, *Soil Sci. Soc. Am. J.*, *65*, 1853–1856.

Houghton, R. A., J. L. Hackler, and K. T. Lawrence (2000), Changes in terrestrial carbon storage in the United States 2: The role of fire and fire management, *Glob. Ecol. Biogeogr.*, *9*, 145–170.

House, J. I., S. Archer, D. D. Breshears, and R. J. Scholes (2003), Conundrums in mixed woody-herbaceous plant systems, *J. Biogeogr.*, *30*, 1763–1777.

Jessup, K. E., P. W. Barnes, and T. W. Boutton (2003), Vegetation dynamics in a *Quercus virginiana - Juniperus ashei* savanna: An isotopic assessment, *J. Veg. Sci.*, *14*, 841–852.

Johnston, M. C. (1963), Past and present grasslands of southern Texas and northeastern Mexico, *Ecology*, *44*, 436–466.

Jolivet, C., D. Arrouays, J. Leveque, F. Andreux, and C. Chenu (2003), Organic carbon dynamics in soil particle size separates of sandy spodosols when forest is cleared for maize cropping, *Eur. J. Soil Sci.*, *54*, 257–268.

Kaiser, K., and G. Guggenberger (2003), Mineral surfaces and soil organic matter, *Eur. J. Soil Sci.*, *54*, 219–236.

Krull, E. G., and S. S. Bray (2005), Assessment of vegetation change and landscape variability using stable carbon isotopes of soil organic matter, *Aust. J. Bot.*, *53*, 651–661.

Krull, E. G., J. O. Skjemstad, W. H. Burrows, S. G. Bray, J. G. Wynn, R. Bol, L. Spouncer, and B. Harms (2005), Recent vegetation changes in central Queensland, Australia: Evidence from $\delta^{13}C$ and ^{14}C analyses of soil organic matter, *Geoderma*, *126*, 241–259.

Laliberte, A. S., A. Rango, K. M. Havstad, J. F. Paris, R. F. Beck, R. McNeely, and A. L. Gonzalez (2004), Object-oriented image analysis for mapping shrub encroachment from 1937 to 2003 in southern New Mexico, *Remote Sens. Environ.*, *93*, 198–210.

Legendre, P., M. R. T. Dale, M. J. Fortin, J. Gurevitch, M. Hohn, and D. Myers (2002), The consequences of spatial structure for the design and analysis of ecological field surveys, *Ecography*, *25*, 601–615.

Liao, J. D., T. W. Boutton, and J. D. Jastrow (2006), Organic matter turnover in soil physical fractions following woody plant invasion of grassland: Evidence from natural ^{13}C and ^{15}N, *Soil Biol. Biochem.*, *38*, 3197–3210.

Loveland, T. R., and R. S. DeFries (2004), Observing and monitoring land use and land cover change, in *Ecosystems and Land Use Change*, *Geophys. Monogr. Ser*, vol. 153, edited by R. DeFries et al., pp. 231–246, AGU, Washington, D. C.

Marriott, C. A., G. Hudson, D. Hamilton, R. Neilson, B. Boag, L. L. Handley, J. Wishart, C. M. Scrimgeour, and D. Robinson (1997), Spatial variability of soil total C and N and their stable isotopes in an upland Scottish grassland, *Plant Soil*, *196*, 151–162.

McAuliffe, J. R. (1994), Landscape evolution, soil formation, and ecological patterns and processes in Sonoran Desert Bajadas, *Ecol. Monogr.*, *64*, 111–148.

McCarthy, J. F., J. Ilavsky, J. D. Jastrow, L. M. Mayer, E. Perfect, and J. Zhuang (2008), Protection of organic carbon in soil microaggregates via restructuring of aggregate porosity and filling of pores with accumulating organic matter, *Geochim. Cosmochim. Acta*, *72*, 4725–4744.

Nobel, J. C. (1997), *The Delicate and Noxious Scrub: Studies on Native Tree and Shrub Proliferation in Semi-arid Woodylands of Austrilia*, CSIRO, Canberra, ACT.

Pacala, S. W., et al. (2001), Consistent land- and atmosphere-based US carbon sink estimates, *Science*, *292*, 2316–2320.

Pannatier, Y. (1996), *VARIOWIN, Software for Spatial Data Analysis in 2D*, Springer, New York.

Rappole, J. H., C. E. Russell, J. R. Norwine, and T. E. Fulbright (1986), Anthropogenic pressures and impacts on marginal, neotropical, semiarid ecosystems: The case of south Texas, *Sci. Total Environ.*, *55*, 91–99.

Rodriguez-Iturbe, I., P. D'Odorico, A. Porporato, and L. Ridolfi (1999), On the spatial and temporal links between vegetation, climate, and soil moisture, *Water Resour. Res.*, *35*, 3709–3722.

Rosenberg, M. S. (2001), *PASSAGE, Pattern Analysis, Spatial Statistics, and Geographic Exegesis, Version 1.1, Dep. of Biol*, Ariz. State Univ., Tempe.

Rouse, J. W., R. H. Haas, J. A. Schell, and D. W. Deering (1973), Monitoring vegetation systems in the Great Plains with ERTS-1, *Proc. Third Earth Resour. Tech. Satell. Symp.*, *1*, 309–317.

Scanlan, J. C., and S. R. Archer (1991), Simulated dynamics of succession in a North-American subtropical *Prosopis*-savanna, *J. Veg. Sci.*, *2*, 625–634.

Scanlon, T. M., J. D. Albertson, K. K. Caylor, and C. A. Williams (2002), Determining land surface fractional cover from NDVI and rainfall time series for a savanna ecosystem, *Remote Sens. Environ.*, *82*, 376–388.

Scholes, R. J., and S. R. Archer (1997), Tree-grass interactions in savannas, *Annu. Rev. Ecol. Syst.*, *28*, 517–544.

SPSS, Inc. (2002), SPSS for Windows, Version 11.5, Chicago, Ill.

Telles, E. C. C., P. B. Camargo, L. A. Martinelli, S. E. Trumbore, E. S. Costa, J. Santos, N. Higuchi, and R. C. Oliviera (2003), Influence of soil

texture on carbon dynamics and storage potential in tropical forest soils of Amazonia, *Global Biogeochem. Cycles*, *17*(2), 1040, doi:10.1029/2002GB001953.

Tilman, D., P. Reich, H. Phillips, M. Menton, A. Patel, E. Vos, D. Peterson, and J. Knops (2000), Fire suppression and ecosystem carbon storage, *Ecology*, *81*, 2680–2685.

Turner, B. L. I., , W. C. Clark, R. W. Kates, J. F. Richards, J. T. Mathews, and W. B. Meyer (Eds.) (1990), *The Earth as Transformed by Human Action: Global and Regional Changes in the Biosphere Over the Past 300 Years*, Cambridge Univ. Press, Cambridge, U. K.

van Auken, O. W. (2000), Shrub invasions of North American semiarid grasslands, *Annu. Rev. Ecol. Syst.*, *31*, 197–215.

van Kessel, C., R. E. Farrell, and D. J. Pennock (1994), Carbon-13 and nitrogen-15 natural abundance in crop residues and soil organic matter, *Soil Sci. Soc. Am. J.*, *58*, 382–389.

Wedin, D. A., L. L. Tieszen, B. Dewey, and J. Pastor (1995), Carbon isotope dynamics during grass decomposition and soil organic matter formation, *Ecology*, *76*, 1383–1392.

Witt, G. B., J. Luly, and R. J. Fairfax (2006), How the west was once: Vegetation change in south–west Queensland from 1930 to 1995, *J. Biogeogr.*, *33*, 1585–1596.

Wu, X. B., and S. R. Archer (2005), Scale-dependent influence of topography-based hydrologic features on patterns of woody plant encroachment in savanna landscapes, *Landscape Ecol.*, *20*, 733–742.

Zitzer, S. F., S. R. Archer, and T. W. Boutton (1996), Spatial variability in the potential for symbiotic N_2 fixation by woody plants in a subtropical savanna ecosystem, *J. Appl. Ecol.*, *33*, 1125–1136.

S. R. Archer, School of Natural Resources, University of Arizona, Tucson, AZ 85721-0043, USA.

E. Bai, Department of Land, Air, and Water Resources, University of California, One Shields Avenue, Davis, CA 95616, USA. (ebai@ucdavis.edu)

T. W. Boutton and X. B. Wu, Department of Ecosystem Science and Management, Texas A&M University, College Station, TX 77843-2138, USA.

F. Liu, Forest Landscape Ecology Laboratory, Department of Forest and Wildlife Ecology, University of Wisconsin-Madison, Madison, WI 53706-1520, USA.